SCIENTIFIC PUBLICATIONS OF THE STATE UNIVERSITY OF NOVI PAZAR
SER. A: APPL. MATH. INFORM. AND MECH. vol. 15, 2, 2023, 61–72

Preisach Mathematical Model of Hysteresis

D. Šumarac, Z. Perović, D. Vatić, T. Curić, I. Nurković, M. Cao

Abstract: Hysteretic nonlinear phenomena occur in many physical processes: ferromagnetism, adsorption, cyclic plasticity in mechanics, phase transformations, economics, etc. It is characterized by the fact that the same instantaneous values of input can give different outputs depending on the history of the input applied. It means that the relationship is not only nonlinear but also multivalued making it very difficult to model and control. In this paper, accent was given to the application to mechanics i.e. to cyclic plasticity of trusses.

Keywords: Preisach model, cyclic plasticity, trusses

1 Introduction

The hysteresis operator is a mathematical concept and it is not directly related to the intrinsic physical causes of hysteresis. Since there are numerous examples of hysteresis phenomena occurring in physical processes (hysteresis in continuum mechanics, in ferromagnetism, in filtration through porous media etc.), appropriate modeling of hysteresis is of great interest to engineers and physicists. One of the most powerful scalar models of hysteresis, among those that are known so far, was proposed by the physicist F. Preisach in 1935 [16] to represent scalar ferromagnetism. There are numerous mathematical models that describe hysteretic behavior and some of them were used to model hysteresis in solid mechanics (Prandt-Ishlikii, Bouc, Wen, Baber-Noori). Application of the Preisach model to cyclic behavior of elasto-plastic material was introduced in 1993 by (Lubarda, Sumarac and Krajcinovic [11],[12]). One of the most important properties of the Preisach operator is the so-called memory map [5], but in addition, it is shown in [11] that suggested (Preisach) model also possesses congruency and wiping out property, which makes this model [11], [12] appropriate to describe the hysteretic behavior of elasto-plastic material. It was also shown that Preisach model can be defined in purely geometric terms [14], without any reference to analytical definition, which is less attractive approach for engineers. Using finite element method, equilibrium equations for structural analysis of trusses are obtained and

Manuscript received August 20, 2023; accepted October 21, 2023.

D. Šumarac, D. Vatić, T. Curić and I. Nurković are with the State University of Novi Pazar, Vuka Karadzića 9, 36300 Novi Pazar, Serbia; Z. Perović is with Faculty of Civil Engineering, University of Belgrade, Serbia, Bulevar kralja Aleksandra 73, 11000 Belgrade, Serbia; M. Cao is with Department of Engineering Mechanics, Hohai University, Nanjing, 210098, China

algorithm for numerical solution is defined in C++ code. Several numerical examples will be presented and results obtained by suggested model are compared with the already existing in the literature. The second and the third part of this paper contains basic outline of the Preisach model and its application of modeling ductile materials subjected to cyclic loading, as explained in [12], [18] and [19]. In the fourth part, finite element equations for static nonlinear analysis of trusses subjected to cyclic loading are shown. In the fifth part, numerical examples are presented and results, obtained by this model, are analyzed and compared with the results obtained by the Bouc-Wen model of hysteresis [3], [21], [7], applied in SAP2000 [4], and results obtained by GP (Generalized Plasticity) model explained in [9].

2 The preisach model of hysteresis

According to Mayergoyz [14], the Preisach model implies the mapping of an input $u(t)$ on the output $f(t)$ in the integral form:

$$f(t) = \iint P(\alpha,\beta) G_{\alpha,\beta} u(t) d\alpha d\beta, \tag{1}$$

where $G_{\alpha,\beta}$ is an elementary hysteresis operator given in Figure 1.a. Parameters α and β are up and down switching values of the input, while $P(\alpha,\beta)$ is the Preisach function. i.e.a weight (Green's) function of the hysteresis nonlinearity to be represented by the Preisach model. The domain of integration of integral (1) is right triangle in the α,β plane, with $\alpha = \beta$ being the hypotenuse and $(\alpha_0, \beta_0 = -\alpha_0)$ being the triangular vertex (Fig.1.b). History of loading corresponds to staircase line $L(t)$ which divides triangle into two parts (Lubarda et al.[11]).

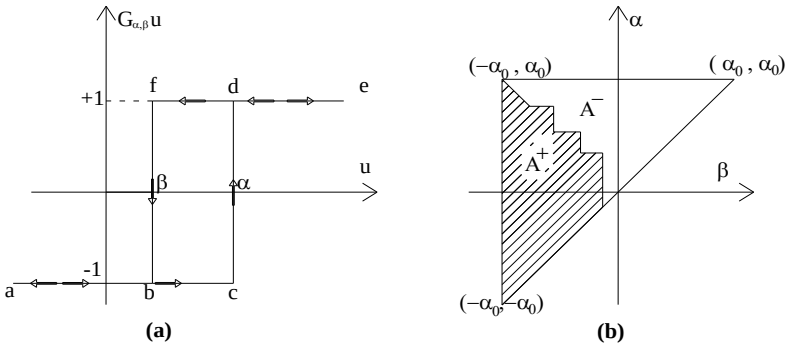

Fig. 1. (a) Elementary hysteresis operator; (b) Staircase line in the Preisach triangle

Maxima or minima of loading history are represented by the vertices with coordinates (α,β) on staircase line $L(t)$ in such a way if the input at a previous instant of time is increased, the final link of $L(t)$ is horizontal, and vice versa if it is decreased it is vertical. Therefore, the triangle is divided into two parts with the positive and negative values of $G_{\alpha,\beta}$ by the interface staircase line $L(t)$. From formula (1) it is obtained:

$$f(t) = \iint_{A^+(t)} P(\alpha,\beta) G_{\alpha,\beta} u(t) d\alpha d\beta - \iint_{A^-(t)} P(\alpha,\beta) G_{\alpha,\beta} u(t) d\alpha d\beta. \tag{2}$$

Denoting the output value at $u = \beta$ by $f_{\alpha,\beta}$ from the limiting triangle, it follows that

$$f_{\alpha,\beta} - f_{\alpha} = -2 \int_{\beta}^{\alpha} \left(\int_{\beta'}^{\alpha} P(\alpha',\beta') \, d\alpha' \right) d\beta'. \tag{3}$$

By differentiating expression (3) twice, with respect to α and β, the Preisach weight function is derived in the form

$$P(\alpha,\beta) = \frac{1}{2} \frac{\partial^2 f_{\alpha,\beta}}{\partial \alpha \partial \beta}. \tag{4}$$

The Preisach model explained above possesses two properties: wiping out and congruency properties. Those properties and much more about Preisach model is explained in the Lubarda et al. [11] and [12].

3 The preisach model for cyclic behavior of ductile materials

One dimensional hysteretic behavior of elasto-plastic material can be successfully described by the Preisach model. Ductile material is represented in various ways by a series or parallel connections of elastic (spring) and plastic (slip) elements Lubarda, at al. [11]. These results have advantage in comparison with classically obtained Iwan, [8], Asaro, [1] because of simplicity and strict mathematical rigorous procedure.Parallel connection of elastic and slip elements, Series connection of elastic and slip elements are discussed elsewhere Sumarac and Stosic, [18], Lubarda, at al. [11]. For understanding this issue, the paper of V. Nikolić at al. [15] can be helpful. Here we will consider a three element unit.

Elastic-linearly hardening material behavior, characterized by the stress-strain curve shown in Fig. 2a. (E and E_h are elastic and hardening moduli respectively), can be modeled by a three-element unit shown in Fig. 2b.

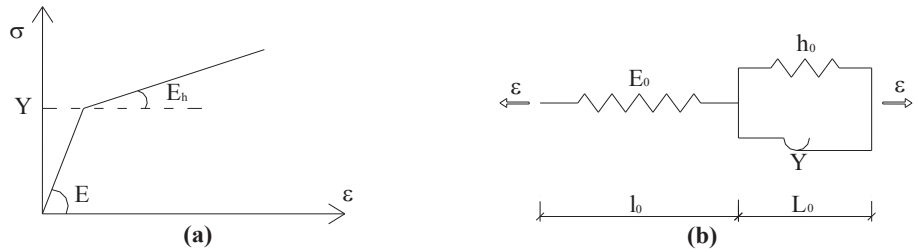

Fig. 2. (a) Elastic-linearly hardening stress-strain behavior with elastic modulus E, initial yield stress Y and hardening modulus Eh;(b) Three-element unit reproducing the stress-strain behavior in (a)

Elastic element of length l and modules E_0 is connected in a series with a parallel connection of elastic and slip element, of length L modulus h_0 and yield strength Y. It then

follows that $E = E_0(l_0 + L_0)/l_0$ and $E_h = E_h(E + h)$, where $h = h_0(l_0 + L_0)/L_0$. Since in this paper, displacement-based finite element method is used where displacement (strain) is unknown variable, only three-element units connected in parallel will be used to model material.

3.1 Three-element unit connected in parallel

In this case the Preisach function can be determined from the hysteresis nonlinearity shown in Fig.2a again, taking into consideration that strain is input and stress is output. The Preisach function in this case has support along the lines $\alpha - \beta = 0$ and $\alpha - \beta = 2Y/E$, i.e. it is given by

$$P(\alpha,\beta) = \frac{E}{2}\left[\delta(\alpha-\beta) + \frac{E-E_h}{2}\delta(\alpha-\beta-2Y/E)\right]. \tag{5}$$

The expression for stress as a function of applied strain is, consequently,

$$\sigma(t) = \frac{E}{2}\left[\int_{-\varepsilon_0}^{\varepsilon_0} G_{\alpha,\alpha}\varepsilon(t)d\alpha - \frac{(E-E_h)}{E}\int_{2Y/E-\varepsilon_0}^{\varepsilon_0} G_{\alpha,\alpha-2Y/E}\varepsilon(t)d\alpha\right]. \tag{6}$$

The first and second term on the right-hand side of (6) are elastic and plastic stress, respectively. For a system consisting of infinitely many of three-element units, connected in a parallel and with uniform yield strength distribution within the range $Y_{\min} \le Y \le Y_{\max}$, the total stress is

$$\sigma(t) = \frac{E}{2}\left[\int_{-\varepsilon_0}^{\varepsilon_0} G_{\alpha,\alpha}\varepsilon(t)d\alpha - \frac{E-E_h}{2}\frac{1}{Y_{\max}-Y_{\min}}\iint_A G_{\alpha,\beta}\varepsilon(t)d\alpha d\beta\right]. \tag{7}$$

In (7) the integration domain A is the area of the band contained between the lines $\alpha - \beta = 2Y_{\min}/E$ and $\alpha - \beta = 2Y_{\max}/E$ in the limiting triangle, shown in Fig.3.b.

3.2 Comparison with experimental results for the strain control uniaxial loading

Stress-strain behavior of material model in plastic domain presented in Fig.3.a is considered to be consisted of two parts, linear and nonlinear.

Nonlinear part of this curve is determined by appropriately adopting stress limits Y_{min} and Y_{max} in addition to elastic modulus E and hardening modulus E_h that defines slope of linear part of strain hardening. By analyzing experimental curve, these parameters could be obtained. For results obtained in experiment of cyclic loading of material in stable cycle loop, published in the paper [10], analytical solution was determined based on model, presented in this paper, of parallel connection of infinitely many elements given in Fig.2b. In this experiment, sample of Titanium alloy was subjected to strain controlled cyclic loadings $\varepsilon = \pm 1.2\,\%$ and stable hysteretic curves were obtained. By analyzing shape of this hysteresis, parameters for material behavior defined in [7] could be determined by considering geometry of experimental curve in Fig.4. Slope of the curve in elastic loading and reloading segments defines modulus of elasticity $E = 114GPa$ and linear part of strain hardening gives hardening modulus $E_h = 17.2MPa$.

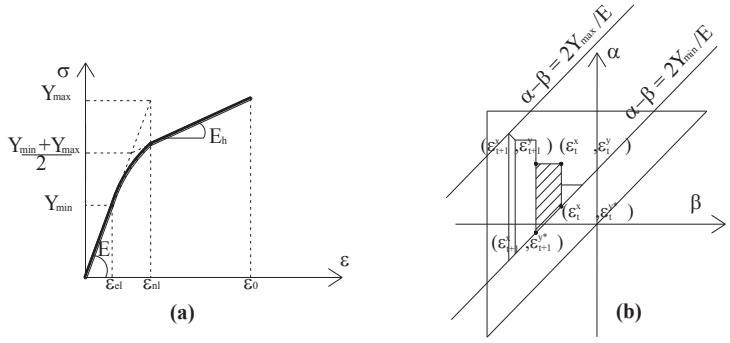

Fig. 3. (a)Stress-strain behavior of material modeled by parallel connection of infinite number of three element units; (b) Set A+(t) of Preisach triangle subdivided into N trapezes.

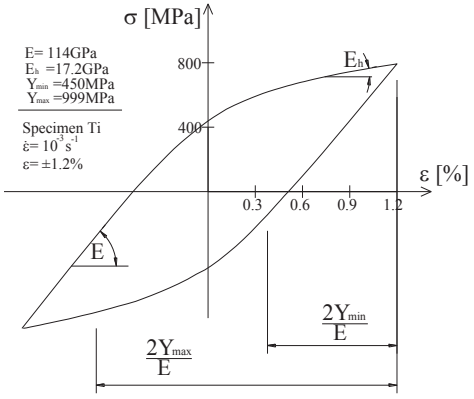

Fig. 4. Results of experiment of cyclic loading of alloy of Tittanium published in [10] and determination of parameters for the Preisach model

If Preisach triangle (Fig.3.b) is analyzed, it can be seen that elastic part of curve's reloading segment always defines constant strain value of $2Y_{min}/E$, while the elastic and nonlinear plastic part of curve's reloading segment give constant strain value of $2Y_{max}/E$. Hence, stress limits $Y_{min} = 450MPa$ and $Y_{max} = 999MPa$ are defined. Experimentally obtained stable cycle loop was in excellent agreement with one obtained using model of parallel connection of infinitely many elements as shown on Fig.5.a. In all numerical examples, presented in this paper, the same material of truss structure is taken and compared with the results obtained by the Bouc-Wen model of hysteresis, one of the most recognizable and probably the model that had the largest application in structural analysis. Therefore parameters for Bouc-Wen hysteresis operator are also determined based on the same experimental results. Detailed formulation and definition of the Bouc –Wen model and its parameters can be found in [3], [21] and [7]. In presented examples, uniaxial case, with no additional possibilities such as degradation and pinching.

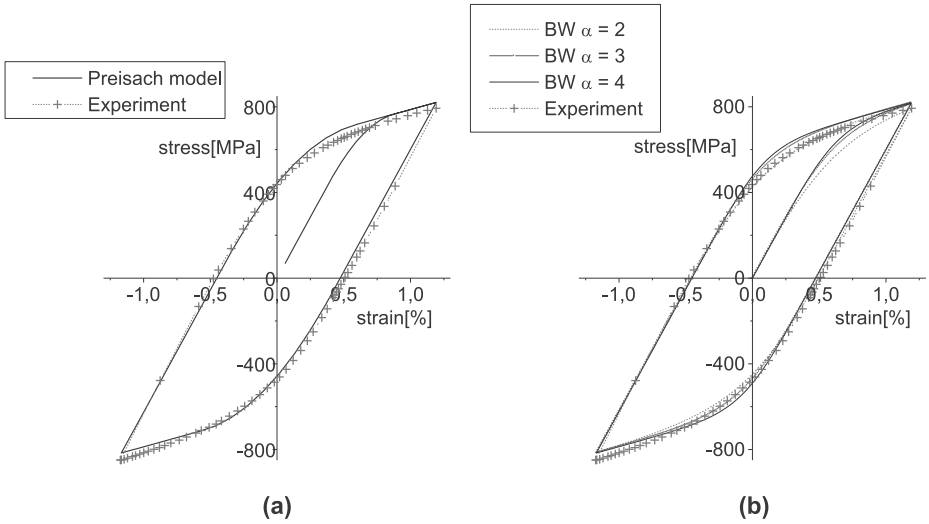

Fig. 5. (a) Comparison of experimentally obtained loop ([10]) with the loop obtained by suggested model of hysteresis; (b) Determination of parameters for the Bouc-Wen model of hysteresis for the best fitting of experimentally obtained loop [10]

effects modeling, is used. All parameters for this model could be determined from experimental results, but the exponent for transition zone was varied to achieve the best approximation of experiment ($\alpha = 3$ gave the best fitting), and results were presented in Fig.5.b.

In addition, results from numerical examples are compared with results obtained by GP finite element [13] based on generalized plasticity material model developed by [9]. GP model has both yield function and limit function and therefore smooth transition between elastic and plastic states is achieved. Material parameters for GP model are also defined from experimental results [10].

4 Finite element equations for trusses subjected to cyclic loading in plastic domain

Using principle of virtual displacements, equations for finite element procedures can be obtained. If only truss elements are considered, (body forces and surface forces are zero), only concentrated loads at nodes, as externally applied load are possible. In the finite element analysis we approximate the structure (in this case truss) as the assemblage of the discrete finite elements interconnected at the nodal points on the element boundaries. The expression for principle of virtual displacements then becomes:

$$\sum_m \int_{V^{(m)}} \bar{\varepsilon}^{(m)T} \sigma^{(m)} dV^{(m)} = \sum_i \bar{u}^{iT} R_C^i, \tag{8}$$

where σ represents stresses in equilibrium with applied loads, R_C^i denotes concentrated forces on point i of applied loads, $\bar{u}^i$ denotes virtual displacements, $\bar{\varepsilon}$ corresponding virtual strains and $m = 1,2\ldots k$, where k is the number of elements (bars). If only one element m of structure is analyzed, substituting equation (7) into (8), it is obtained:

$$\int_V \bar{\varepsilon}^T \frac{E}{2}\left[\int_{-\varepsilon_0}^{\varepsilon_0} G_{\alpha,\alpha}\varepsilon(t)d\alpha\right]dV -$$

$$-\int_V \bar{\varepsilon}^T \left[\frac{E\,(E-E_h)}{4}\frac{1}{Y_{\max}-Y_{\min}}\iint_A G_{\alpha,\beta}\varepsilon(t)d\alpha d\beta\right]dV = \bar{u}^T R_C. \tag{9}$$

It was demonstrated in [12] and [18] that for corresponding strain limits $\varepsilon_{el} = Y_{\min}/E$ and $\varepsilon_{nl} = Y_{\max}/E$, Preisach triangle is formed as presented in Fig.3.(b). It is shown in [11] and [12] that the first part of the expression in Eq.(7) represents elastic stress of axially loaded bars. The second part of the expression in Eq.(7) defines plastic stress, when strain in material exceeds elastic limit ($\varepsilon > \varepsilon_{el}$) and by geometric interpretation it is shown in [11] and [12], that it actually represents difference of integrals over positive and negative area $A^+(t)$ and $A^-(t)$ in the Preisach triangle. It is obvious that area $A^+(t)$ is consisted of sum of N trapezes whose vertices have coordinates equal to past input extrema [11], and therefore it represents function of predominant input strain data values $\left(\varepsilon_t^x, \varepsilon_t^y\right)$ (Fig.3.b):

$$A^+(t) = \sum_{t=1}^{N}\left[\left(\varepsilon_{t+1}^x - \varepsilon_t^x\right)\left(\varepsilon_{t+1}^y - \varepsilon_{t+1}^{y^*} + \varepsilon_t^y - \varepsilon_t^{y^*}\right)/2\right]. \tag{10}$$

Considering that displacement-based finite element method is used, it is necessary to exchange strain variable ε with bar length change Δu, and because of Eq.(10), $A^+(t)$ will therefore represent function of predominant input bar length change data values Δu. Second part of the equation (10) then becomes:

$$\iint_A G_{\alpha,\beta}\times\varepsilon(t)\times d\alpha d\beta = \iint_{\bar{A}} G_{\bar{\alpha},\bar{\beta}}\times\Delta u(t)\times d\bar{\alpha}d\bar{\beta} = A^+(t) - A^-(t) = \frac{1}{L^2}\times u_{pl} = \varepsilon_{pl}, \tag{11}$$

where ε_{pl} and u_{pl} represent differences of positive and negative sets in the Preisach triangles where strain and bar length change are used as input functions, respectively. L represents bar length. Substituting Eq.(11) in (9), (12) is obtained:

$$\bar{u}^{(m)T}\left[\int_{V^{(m)}} B^{(m)T}EB^{(m)}dV^{(m)}\right]\bar{u}^{(m)} -$$

$$-\bar{u}^{(m)T}\left[\int_{V^{(m)}} B^{(m)T}\frac{E\,(E-E_h)}{4\,(Y_{\max}-Y_{\min})}\frac{1}{\left(L^{(m)}\right)^2}dV^{(m)}\right]\cdot u_{pl}^{(m)} = \bar{u}^{(m)T}R_C^i. \tag{12}$$

It is considered that this problem would not require large displacement and large strain analysis, and if strain displacement matrix B is introduced, expressions in brackets of first

and second part of (11) are actually defining elastic stiffness matrix and plastic stiffness matrix respectively:

$$K_{el}{}^{(m)}\bar{u}^{(m)} - K_{pl}{}^{(m)} \cdot u_{pl}^{(m)} = R_C^i. \tag{13}$$

For the finite element assemblage, expression in Eq.(11) becomes

$$K_{el}U - K_{pl} \cdot U_{pl} = R. \tag{14}$$

It is important to emphasize that elements of vectors U represent nodal displacements of the global system while elements of vector U_pl represent differences of positive and negative sets $A^{(+t)}$ and $A^{(-t)}$ in corresponding Preisach triangle, transformed in global system. For solving problem of nonlinear static analysis, iterative procedure using Newton-Raphson initial stress method can be applied:

$$\begin{aligned} K_{el}\Delta U^{(i)} &= {}^{t+\Delta t}R - {}^{t+\Delta t}F^{(i-1)} \\ {}^{t+\Delta t}U^{(i)} &= {}^{t+\Delta t}U^{(i-1)} + \Delta U^{(i)} \\ {}^{t+\Delta t}F^{(i)} &= K_{el}{}^{t+\Delta t}U^{(i)} + K_{pl}{}^{t+\Delta t}U_{pl}{}^{(i)}. \end{aligned} \tag{15}$$

Procedure for iteration i in Eqs.(15) is repeated until convergence is achieved. According to defined procedures for numerical analysis from Eqs.(13) to (16), algorithm for elastoplastic analysis of trusses subjected to cyclic loading was defined in C++ code. During every step and iteration in expressions (13) to (15), in every bar of truss structure, plastic part from Eq.(15) is being calculated according to current state of corresponding bar and then assembled in global matrix in Eq.(14). For assigned material properties, corresponding stress-strain behavior obtained by the Preisach model can be presented as shown in Fig.3.a, where ε_{el} is elastic strain limit of material, ε_{nl} is plastic strain limit at the onset of linear hardening and ε_0 is optional maximum strain limit of material. In static analysis, if material has very small or no strain hardening $E_h \approx 0$, in order to provide some indication of when both the displacements and the forces are near their equilibrium values, it is recommended [2] that convergence criteria should be based on energy tolerance condition as shown in Eq.(16). In every iteration increment of internal energy is compared to initial internal energy increment:

$$\Delta U^{(i)T}\left({}^{t+\Delta t}R - {}^{t+\Delta t}F^{(i-1)}\right) \leq \in_E \left(\Delta U^{(1)T}\left({}^{t+\Delta t}R - {}^{t}F\right)\right). \tag{16}$$

5 Numerical examples

In all numerical examples, material properties for all truss bars are taken from experimental results [10], shown in paragraph 3.2. In order to outline the advantages of the Preisach hysteresis operator, results from presented model were compared to the results of the Bouc-Wen and GP model.

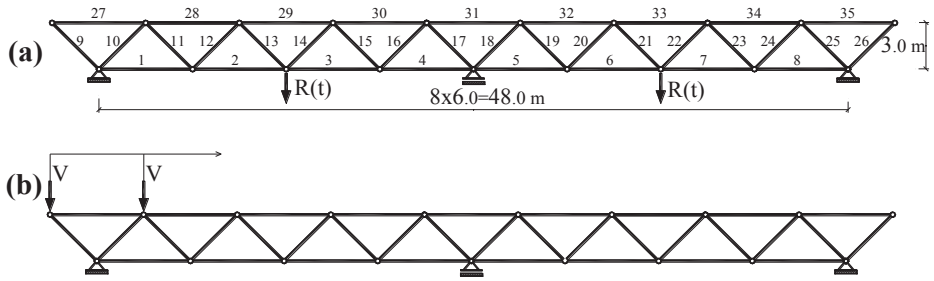

Fig. 6. (a) Geometry and loading R(t) of truss structure for the first numerical example (b) Moving load V in the second numerical example

5.1 Quasi-static analysis of two-span truss without damage

In the first example, truss structure shown in Fig.6.a is analyzed under two types of load (Fig.6.a and Fig.6.b). The first load case $(R(t))$ has cyclic character and its input function is shown in Fig.11.b, while in the second case truss was subjected to moving load pattern of two concentrated forces $2xV(V = 8000kN)$. Structure consists of two types of bars. Horizontal bars with length of $6m$, and cross section areas $A_{hor} = 0.02m^2$ and diagonal bars with cross section areas $A_{dia} = 0.015m^2$.

In the first case of loading, all bars of structure, which undergo plastic deformation, have stable hysteretic loops and resulting stress-strain diagram for some of characteristic bars $(29, 31)$ are presented in Fig. 7.

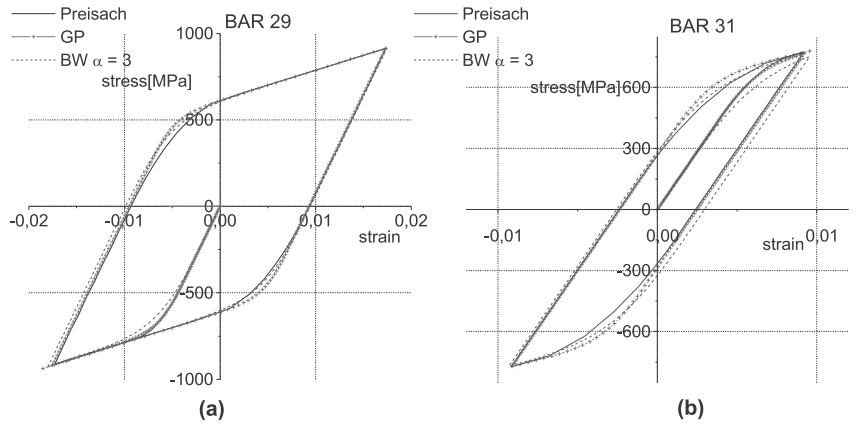

Fig. 7. Stress strain hysteresis curves for the first numerical example: Comparison of the Preisach model, GP model and the Bouc-Wen model (alpha=3) for bar 29 (a) and bar 31 (b) respectively

Although in the second case applied moving load pattern $2xV$ doesn't have cyclic character, bars will be subjected to load reversals, since these concentrate forces move across two span of continuous truss structure. Structure is subjected to five consecutive cycles of moving load pattern (Fig.6.b). Note that bars whose position is symmetrical around midpoint of structure should have identical response, according to position of load, in case of

elastic analysis. However, all bars of the structure are being plastically deformed gradually and therefore symmetrical bars have different deformed state at same instant of time of loading and therefore different strain history. Results according to different models are presented in Fig.8, where maximum absolute vertical displacement during each cycle and residual maximum vertical displacement after each cycle are presented and compared. When results obtained using the Preisach model are analyzed, it can be seen that loading after first cycle doesn't increase deformation significantly. In summary, after the second and all subsequent cycles, identical and stable deformation is observed and there is no further significant increase of plastic strain as it is shown in Fig.9.

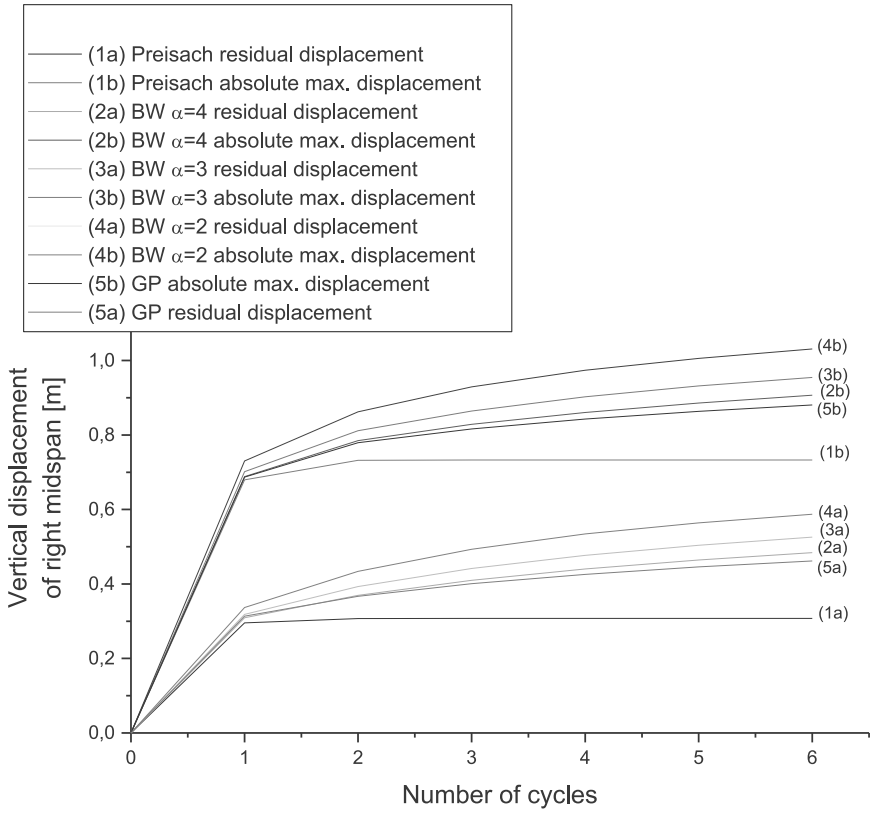

Fig. 8. Maximum absolute vertical displacement of the right midspan of truss during each cycle and residual maximum vertical displacement after each cycle in the second numerical example obtained using different models

The most obvious difference between Preisach model and the Bouc-Wen model, can be seen after analyzing of resulting hysteresis. While resulting loops obtained by the Preisach model are decreased significantly after first cycle, providing elastic shakedown behaviour, that is not the case with corresponding results of the Bouc Wen and GP model. Hence, when results of the Bouc-Wen and GP model of hysteresis are compared, it can be seen that stabilization of plastic deformation in second numerical example occurred in higher

number of cycles and higher strain values as shown in Fig.9.

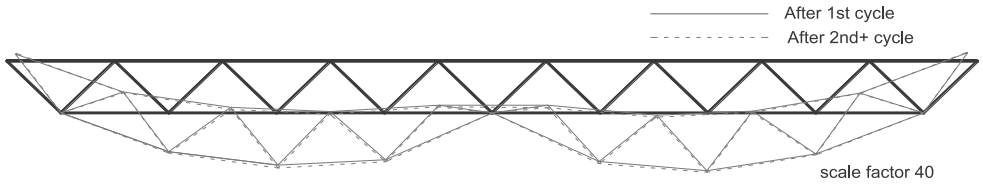

Fig. 9. Deformed shape of structure for the second numerical example, obtained by suggested model, (scale factor = 40) after first cycle and after 2nd and all subsequent cycles

6 Conclusion

In the present paper it is shown that the Preisach model of hysteresis can be successfully applied in structural analysis of trusses, besides previously shown advanced application in the case of uniaxial cyclic loading of bar [11],[12] and cyclic bending of beam [18],[19]. Program in C++ code using finite element procedure is made for analyzing static and dynamic problems of trusses subjected to cyclic loading in the plastic range. The procedure leads to Newton-Raphson's initial stress method. Damage can be included in presented algorithm by introducing scalar damage variable and basic concepts of continuum damage mechanics. It is also shown that the Preisach model can be defined in purely geometric terms, without any reference to analytical definition. Results obtained by this model were compared with the results from the Bouc-Wen and the GP (Generalized Plasticity) models for several numerical examples. Even the agreement of the obtained results is excellent, this model has several advantages. The analytical solution in closed form provides mathematical rigor of the Preisach model, while its absolute equivalent geometric interpretation enables numerical effective solution and less computational cost. Considering all the possibilities that Preisach model poses, this type of analysis in finite element procedures is yet to be applied.

References

[1] R. J. Asaro, *Elastic-plastic memory and kinematic type hardening,* Acta Metall. **23**, 1255-1265 (1975)

[2] K. J. Bathe, *Finite Element Procedures,* Prentice Hall (1996)

[3] R. Bouc, *Modèle Mathématique d'Hystérésis*, Acustica, 24, 16—25, (1971) (in French)

[4] CSI Analysis Reference Manual for SAP2000, ETABS, SAFE and CSiBridge, Computers and Structures Inc., (2009)

[5] S. Erlicher, *Hysteretic degrading models for the low-cycle fatigue behavior of structural elements, Theory, Numerical aspects and Applications*, Dottorato di ricerca in Modellazione, Conservazione e Controllo dei Materiali e delle Strutture, Universita Degli studi di Trento, (2003)

[6] S. Erlicher, N. Point, *Endochronic theory, nonlinear kinematic hardening rule and generalized plasticity: A new interpretation based on generalized normality assumption*, International Journal of Solids and Structures, 43, 4175-4200, (2006)

[7] M. Ismail, F. Ikbouane, J. Rodellar, *The Hysteresis Bouc-Wen model*, a Survey, Arch Comut Methods Eng,16,161-188, (2009)

[8] W. D. Iwan, *On a class of models for the yielding behavior of continuous and composite systems*, J. Appl. Mech., 34, 612-617 (1967)

[9] S. Kostic, F. Filippou, C. L. Lee, *An efficient beam-column element for inelastic 3D frame analysis*, Computational Methods in Applied Sciences, 30, 49-67, (2013).

[10] D. Kujawski, E. Krempl, *The Rate (Time)-Dependent Behaviour of Ti-7Al-2Cb-1Ta Titanium Alloy at Room Temperature Under Quasi Static Monotonic and Cyclic Loading*, J. Appl. Mech., 48, 55-63 (1981)

[11] A. V. Lubarda, D. Sumarac, D. Krajcinovic, *Hysteretic response of ductile materials subjected to cyclic loads*. In: Ju, J.W. (ed.) Recent Advances in Damage Mechanics and Plasticity, ASME Publication, AMD, 123, 145-157 (1992)

[12] A. V. Lubarda, D. Sumarac, D. Krajcinovic, *Preisach model and hysteretic behavior of ductile materials*. Eur. J. Mech., A/Solids, 12, (4), 445-470 (1993)

[13] J. Lubliner,RL. Taylor, F. Auricchio, *A new model of generalized plasticity and its numerical implementation* , International Journal of Solids and Stuctures 30(22):3171-3184, (1993)

[14] I. D. Mayergoyz, *Mathematical Models of Hysteresis*, Springer-Verlag, New York (1991)

[15] V. Nikolić, D. Djekić, A. Radakovic, Dž. Pučić, *Numerical Methods for Solving the Dynamic Behavior of Real Systems* Scientific Publications of the State University of Novi Pazar, Series A: Applied Mathematics, Informatics and Mechanics, vol. 6, no. 1 (2014), p.25-34

[16] F. Preisach, *Über die magnetische Nachwirkung*, Z. Phys., 94, 277-302 (1935)

[17] Yu. N. Rabotnov, *Elements of Hereditary Solid Mechanics*, Mir Publishers, (1980)

[18] D. Sumarac, S. Stosic, *The Preisach model for the cyclic bending of elasto-plastic beams*, Eur. J. Mech., A/Solids 15 (1), 155-172 (1996)

[19] D. Šumarac, Z. Petrašković, *Hysteretic behavior of rectangular tube (box) sections based on Preisach model*, Archive of Applied Mechanics, 82 (10), 1663-1673(2012)

[20] A. Visintin, *Mathematical Models of Hysteresis*, Dipartimento di Matematica dell'Universita degli Studi di Trento, Italia, (2005)

[21] Y. K. Wen, *Method for Random Vibration of Hysteretic Systems*, Journal of the Engineering Mechanics Division, Proc. ASCE, 102, 249—263, (1976)